

## Enhanced thermal stability of “environmentally friendly” biodegradable poly(lactic acid) blends with cellulose acetate. An experimental and molecular modeling study

Ahmed H. Ibrahim<sup>1,2</sup>, Amina A. F. Zikry<sup>2</sup>, Tarek M. Madkour<sup>1,\*</sup>

<sup>1</sup> Department of Chemistry, The American University in Cairo, AUC Avenue, P.O. Box 74, New Cairo 11835, Egypt

<sup>2</sup> Department of Chemistry, Helwan University, Ain-Helwan, Cairo 11785, Egypt

\*corresponding author e-mail address: [tarekmadkour@aucegypt.edu](mailto:tarekmadkour@aucegypt.edu)

### ABSTRACT

Cellulose acetate (CA) is added to the “Environmentally friendly” poly(lactic acid) (PLA) to improve its materials stiffness and thermal stability for use in various applications. Stress-strain showed that small amounts of CA had contributed to PLA flexibility while maintaining high values for the stress. The improved mechanical properties of the samples signifies the stability of the blend due to the formation of 3D-hydrogen bonding network between the CA and PLA chains as indicated by FTIR analysis. Extended thermal degradation highlighted the susceptibility of neat PLA chains to degradation over extended periods of time. The presence of CA component protected PLA chains as a result of the crosslinking between the resultant free radicals and the polymeric chains, which increased the molecular weight of the samples and its overall toughness. Molecular simulations showed that enthalpy of mixing had positive values at low temperatures indicating blend instability as the entropic contribution to free energy of mixing was not sufficient to overcome the enthalpic-driven phase separation. Greater free energy values at higher PLA content coincided with the experimental observation that blends with high PLA content showed appreciable mechanical response whereas those with higher CA content showed no mechanical integrity as predicted by molecular modeling.

**Keywords:** *poly(lactic acid); cellulose acetate; biodegradable polymers; mechanical properties; molecular modeling; free energy of mixing.*

### 1. INTRODUCTION

Poly(lactic acid) (PLA) has emerged as one of the most promising “environmentally friendly” biodegradable candidates in replacing conventional petroleum-based polymers [1]. General advantages of petroleum-based polymers include low cost, high-speed production and good mechanical performance. Alternatively, they show many different disadvantages such as declining oil and gas resources, environmental concerns, uneconomical costs, cross-contaminations during their recycling and consumer toxicity risks associated with the migration of unreacted monomers, free radicals and various additives to edible materials.<sup>[2]</sup> Biopolymers, however, are naturally safe and their biodegradation generally involves natural products and by-products, which contributes to biomass and could be used for the production of nutrients, fuel and fertilizers.

PLA is a biodegradable polymer with participation in a wide range of industrial applications as a result of its unique properties such as high mechanical strength, good appearance, low toxicity and good barrier properties. PLA, however, shows some properties such as inherent brittleness and low thermal stability, which hinders its large scale-application in the polymer industry and pose considerable scientific challenges [3], [4]. A great number of researchers have studied the different properties of PLA alone or in combination with other polymers either through blending or copolymerization [2].

PLA degradation takes place through the simple hydrolysis of the ester bond, which depends on size and shape of the sample

as well as the hydrolysis temperature [5], but is independent on the presence of enzymes as a precondition for its catalysis. PLA thermal degradation consists predominantly of two main mechanisms, (i) random main-chain scission and (ii) unzipping depolymerization reactions [6]. The random degradation mechanism may involve a combination of the oxidative degradation, cis-elimination, intramolecular and intermolecular trans-esterification reactions in addition to the aforementioned ester-bond hydrolysis [7]–[9]. Random main-chain scission at temperatures above 180°C have shown to affect the melt degradation of PLA [10]. Nevertheless, other active byproducts of these processes such as residual monomers, and chain-end groups as well as other impurities were found to accelerate the thermal degradation of PLA [11], which result in an undesired molecular weight reduction accompanied by a weight loss that occurs from 180°C to 220°C. Modification of the polymer using chain extenders to afford long and branched structures was reported as to control the degradation of PLA [6]–[13]. In this approach, using a chain extender is thought to reconnect cleaved chains and subsequently maintaining the molecular weight of the polymer and its overall mechanical integrity [14]–[18]. Multi-functional epoxy compounds were used in this approach due to their ability to react with nucleophilic end group's such as OH and COOH groups of PLA. Branched but less cross-linked PLA could be also obtained with using more than 1.5% by wt. of a multifunctional epoxide [19], [20]. The branched polymers not only increase the molecular

weight, but possess other properties when compared with linear polymers. The addition of such a chain extender may have enhanced the long-term usage of PLA but the formation of crosslinked or branched polymeric chain will definitely hinder the extrusion and injection formability of PLA due to the increase in the polymer viscosity which will require the use of higher temperatures to control the increase in the processing viscosity [21], [22]. Similar chain extenders were also sought for crystalline PLA as well as for amorphous ones [23].

Even though replacing petroleum-based plastics with environmentally friendly biodegradable polymers such as PLA is considered one of the most important scientific and economic issues, the improvement in the polymeric flexibility and thermal stability is an essential step for this transition. Usually, the presence of fillers improves the elastic modulus of the polymer although decreases its elongation at break. In case of PLA, the

polymer modulus is quite high due to the apparent stiffness of the polymer but its extensibility is quite limited and is reduced even further with the addition of these filler particles. Interestingly, it was also reported [24] that the elastic modulus of PLA composite with microcrystalline cellulose was smaller than that of the composite with the same amount of bentonite. A decrease in the molar mass and weight loss of PLA composites with fillers and/or fibers of natural origin was observed [25]–[28] whereas man-made cellulose fibers and nanofibers had their molar mass increased [27]–[29]. Progress in the field of polymer composites and nanocomposites with biodegradable fillers and fibers was a subject of a recent review [30]. Biodegradable blends of PLA with cellulose acetate (CA), another biodegradable polymer, are thus considered in this work as a possible route for the improvement of both the flexibility and overall thermal stability of this important polymer.

## 2. EXPERIMENTAL SECTION

**2.1. Materials.** Poly (lactic acid) (PLA) pellets with a commercial name “Ingeo” grade 4043D of density 1.24 g/cc, relative solution viscosity (RV) of 4.0 (+/- 0.10), and D-Isomer level of 4.35% (+/- 0.55%) was purchased from Nature Works LLC, Minnetonka, USA. Cellulose acetate (CA) powder with commercial name “cellulose acetate” of density 1.24 g/cc was purchased from Loba Chemie, India. The PLA pellets were dried under vacuum at 40°C and 600 mbar for 5 hours. Finally, 1, 4- Dioxane (spectrophotometric grade  $\geq 99$ , Mwt. 88.11) was purchased from Tedia, USA and used as is without further purification.

**2.2. Preparation of the polymeric films.** In order to investigate the mechanical and thermal properties of PLA/CA blends, different films for each blend composition was prepared using solvent casting method. 10 g of the total polymer content was dissolved in 90 g 1,4-dioxane using magnetic stirrer for 8 hours at 40°C. The polymeric solution was then casted on a smooth, free of scratches glass plates using a laboratory-designed applicator. The initial thickness of each film was between 0.5-0.65 mm. The cast films were kept in a closed environment to avoid formation of air bubbles or film deformation. The films were allowed to sit for 24 hours at room temperature and then were subjected to vacuum distillation at 50°C and 600 mbar for 24 hours to remove any traces of the residual solvent, which otherwise may act as a plasticizer and could eventually distort the film properties. Various PLA/CA film compositions of 100/0, 95/5, 90/10, 85/15, 80/20, 75/25, 70/30, 60/40, 50/50, 40/60 and 0/100 were thus prepared to complete this study. In each case the total amount of the polymer content used in the preparation of each film was 10 g, i.e. in case of 80/20 composition, 8 g of PLA were mixed with 2 g of CA and were all dissolved in 90 g 1,4-dioxane as described above. Needless to say, 100/0 composition refers to neat PLA polymer and 0/100 refers to neat CA polymer.

**2.3. Fourier-Transform Infra-Red analysis (FTIR).** Thermo-Scientific, Nicole 380 FT-IR was used to reveal and confirm the chemical structures of the prepared samples and possible shifts in the IR spectra due to the formation of any hydrogen bonding

between PLA and CA. The films were cut into 2 cm x 2 cm with thickness of 0.7 mm. FTIR measurements were obtained by averaging 32 scans at resolution of 4 cm. All the prepared samples were analyzed in the wavelength range from 500-4000  $\text{cm}^{-1}$  wavenumber.

**2.4. Thermogravimetric analysis (TGA).** TGA experiments were carried out to determine the variation in the thermal degradation temperature of the various films using TGA analyzer (Thermo Scientific - TGA/FTIR, Q Series). Heating rate of 10°C  $\text{min}^{-1}$  was used to raise the temperature of 10-14 mg samples from room temperature up to 500°C under nitrogen purge flow rate of 50 ml  $\text{min}^{-1}$ . The precision of the temperature measurement was less than 0.5°C.

**2.5. Stress-strain measurements.** The stress-strain isotherms of the various samples at room temperature were obtained on the dumbbell-shaped specimens cut from the cast sheets. Each sample was held vertically between two clamps with the lower clamp fixed and the upper clamp suspended from a strain gauge (Statham model G1-16-350). A constant voltage DC power supply (Hewlett Packard 6217) was used to supply approximately 14 volts potential to the transducer and was connected to DS1M12 digital oscilloscope & WaveForm generator for output data recording. The transducer was frequently calibrated using a set of standard weights. Its output was found to remain constant over the usual time span of an experiment. Prior to attaching the clamps to a sample, two thin lines were drawn on it. The exact length of the thus-demarcated section of the sample was measured precisely at the desired temperature by means of a cathetometer (Gaertner Scientific Corp., Model M940-303P, precision 1 micron), and the thickness and width were determined with a micrometer. Three measurements each along the thickness and width of the strip were taken, and the average cross-sectional area,  $A^*$ , was determined after complete evaporation. The upper clamp was raised to a position giving the desired elongation of the strip in a step-wise fashion. The distance between the two lines was measured with a cathetometer and recorded as the length L. The ratio of L to  $L_0$

(initial length) presents the elongation (strain),  $\alpha$ . The potential from the stress gauge was calibrated in terms of Newtons (N). The stress-strain measurements were made using a sequence of increasing values of the elongation. The equilibrium elastic force,  $f$ , was noted after the force reading has become sensibly constant for at least 15 min. The elastic quantity of interest for the stress-strain investigation portion was the nominal stress,  $f^*$ , defined by:

$$f^* = N / A^* \quad (1)$$

**2.6. Dry thermal degradation test.** In order to test the degradability of the prepared blends, the oven method was used in accordance with ASTM 0573-99. Specimens for degradation were placed in an air oven preheated to 100°C and in one circumstance up to 50°C. The specimens were subjected to the thermal degradation treatment for 1, 2, 3, 4 and 5 days. Additionally one sample was tested at 50°C for 4 hours. After degradation, the specimens were removed from the oven, cooled to room temperature on a flat surface and allowed to stand for not less than 24 hours prior to further testing.

**2.7. Theoretical Methodology.** Molecular models of the various polymeric blends were constructed and investigated using the BLENDS module in Materials Studio® simulation package available from Accelrys, Inc, UK. The simulation study was used to investigate on a molecular-level the influence of temperature on the free energy of mixing two polymeric materials and to generate phase diagrams for various blend systems.

The modeling work is based on Flory-Huggins model [31]–[33]. The general expression for the free energy of mixing of a binary system is:

$$\frac{\Delta G}{RT} = \frac{\phi_b}{\phi_b} \ln \phi_b + \frac{\phi_s}{\phi_s} \ln \phi_s + \chi \phi_b \phi_s \quad (2)$$

where  $\Delta G$  is the free energy of mixing (per mole),  $\phi_i$  is the volume fraction of component  $i$ ,  $n_i$  is the degree of polymerization of component  $i$ ,  $\chi$  is the interaction parameter,  $T$  is the absolute

temperature and  $R$  is the gas constant. The first two terms represent the combinatorial entropy. This contribution is always negative, hence favoring a mixed state over the pure components. The last term is the free energy due to interaction. If the interaction parameter,  $\chi$ , is positive, this term disfavors a mixed state. The balance between the two contributions gives rise to various phase diagrams.

The interaction parameter,  $\chi$ , is defined as:

$$\chi = \frac{E_{mix}}{RT} \quad (3)$$

where  $E_{mix}$  is the mixing energy, which is the difference in free energy due to interaction between the mixed and the pure state. PLA/CA 80/20 blend was thus simulated and minimized using the molecular modeling technique as shown in figure 1.

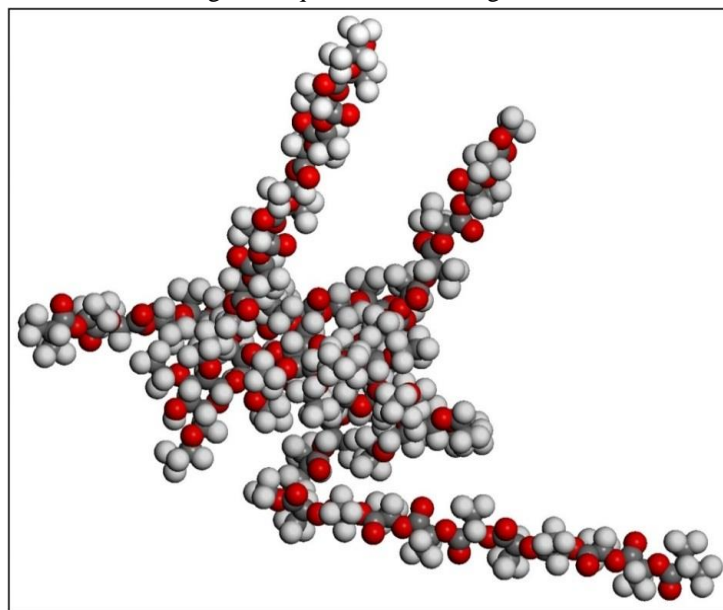


**Figure 1.** Schematic representation of a molecular model of PLA/CA blend.

### 3. RESULTS SECTION

**3.1. Fourier-Transform Infra-Red spectroscopy (FTIR).** The presence of hydrogen bonding between OH groups on CA and the C=O groups of PLA is evident by FTIR spectra, figure 2, which act as to stabilize the polymer blend at normal conditions. The presence of hydrogen bonding also has two major influences on the spectra. Firstly, its presence causes a shift toward lower frequency of all function groups involved in the hydrogen bonding. This is interesting when considering the methyl C-H bending at 2850-2995  $\text{cm}^{-1}$  and the C=O stretch band at 1670-1730  $\text{cm}^{-1}$ . The greater the amount of CA, the greater shifting of the C=O stretch band as is observed. Secondly, the peaks are generally broadened as is observed for the C=O stretch band.

**3.2. Thermal gravimetric analysis of the various blend films.** TGA thermograms of the various PLA/CA blend films (100/0, 95/5, 90/10, 85/15, 80/20 and 0/100) are all shown in figure 3. The figure clearly shows that the degradation takes place between 317°C and 385°C for all the samples. All samples show steady degradation behavior as a common feature. The process of

degradation is qualitatively characterized by a set of temperature points on the TGA curve, shown in Table 1. Upon heating, the sample commences the degradation stage at temperature  $T_1$  and reaches its maximum value a temperature  $T_2$  with weight loss percentage (wt loss %) at the end of that stage.

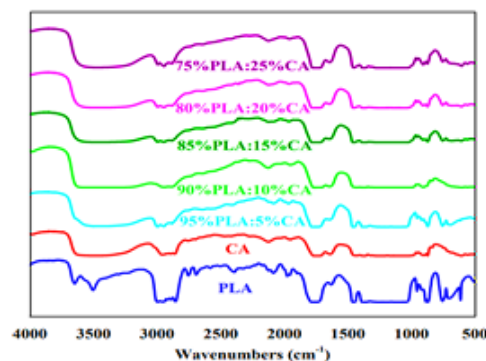


**Figure 2.** FTIR spectra of various PLA/CA blends with different compositions.

It is a quite interesting to observe the complete conversion of pure PLA sample into all volatile compounds with 0% residue remaining at the end of the thermal degradation process in contrast to the CA and PLA/CA blends which small amount of residues in a form of incomplete burning of carbon ashes remained at the end of the degradation process.

It is obvious from the table and the figure that the onset temperature of the degradation process as indicated by  $T_1$  temperature for the various polymer blend samples were influenced to a small extent due to the presence of an increasing amount of CA.

This could be explained on the basis of the high  $T_1$  temperature (331°C) for the CA polymer than that of PLA (317°C), which resulted in the gradual increase of  $T_1$  with the increase of the CA content in the blends.

**Table 1.** Thermogravimetric analysis data of PLA/CA blends with various compositions.

PLA/CA	$T_1$ min (°C)	$T_2$ max (°C)	Weight loss %
100/0*	317	365	100
95/5	312	360	85
90/10	328	371	82
85/15	322	380	79
80/20	330	378	72
75/25	322	381	69
0/100**	331	385	85

\*Neat PLA

\*\*Neat CA

**3.3. Stress-strain measurements.** Stress-strain isotherms for typical PLA/CA blends in comparison to that of neat PLA are shown in figure 4 by plotting  $f^*$  against the elongation,  $\alpha$ , for these blends. It is obvious from the figure that the addition of small amount (5%) of CA to PLA has actually increased the stiffness of PLA as manifested by the higher nominal force at lower elongations.

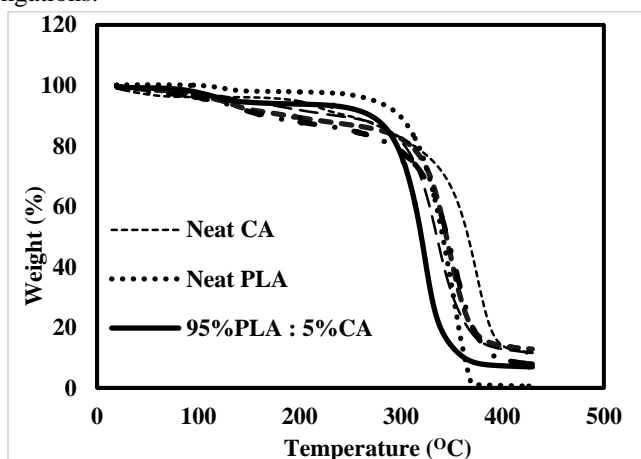


**Figure 3.** TGA thermograms of various PLA/CA blends with different compositions.

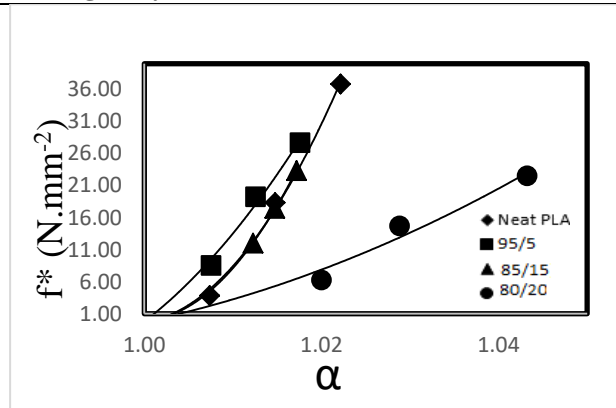


**Figure 4.** Stress-strain isotherms of the various PLA/CA blends.

Higher percentage of CA (20%) has actually contributed tremendously to the flexibility of PLA while maintaining high values for the stress and thus leading to the toughness of these blends. Further increment in the CA concentration has led to the worsening of the mechanical response of these blends and at 50% composition the samples have completely failed the stress-strain test. The improved flexibility of 20% CA blend actually signifies the stability of the blend possibly due to the formation of hydrogen bonding 3D network between CA and PLA chains as indicated by FTIR spectral analysis. At higher CA concentrations, the repulsive forces between the two polymers increase greatly up to the point that they could not be stabilized by the formation of the hydrogen bonds.

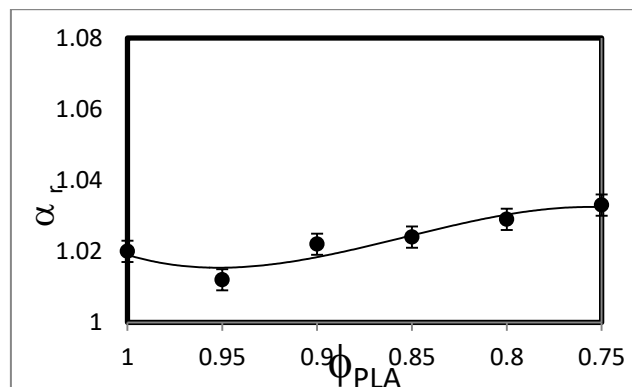


**Figure 5.** The influence of PLA/CA blend composition on the elongation at rupture.

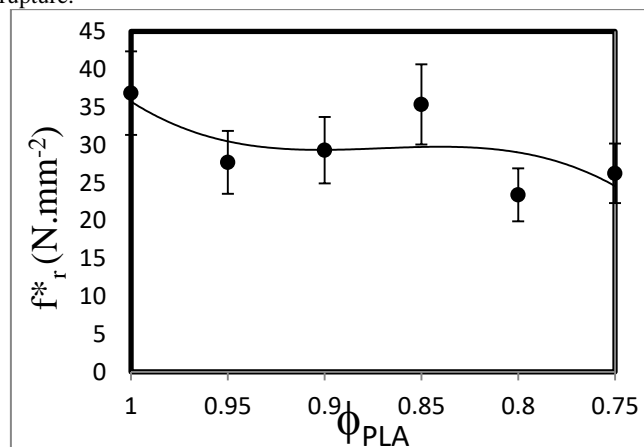


**Figure 6.** The influence of PLA/CA blend composition on the nominal force at rupture.

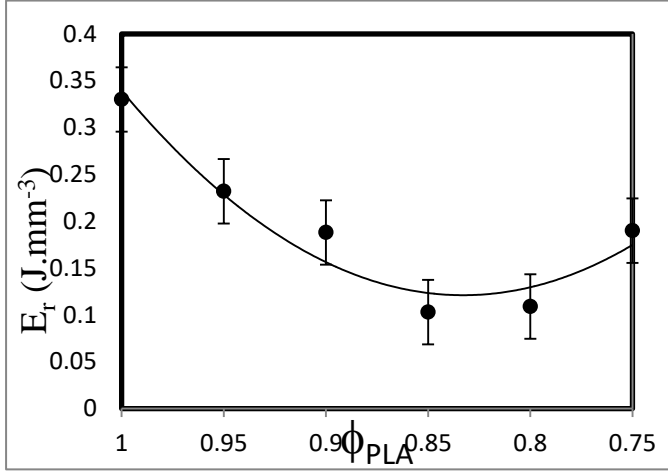


**Figure 7.** The influence of PLA/CA blend composition on the energy required to rupture the sample. To elaborate on these findings further.

**Table 2.** Ultimate mechanical properties of the PLA/CA blends with various compositions.

PLA/CA	$\alpha_r$	$f_r^*$ (N.mm <sup>-2</sup> )	$E_r$ (J.mm <sup>-3</sup> )
100/0	1.020	36.84	0.330
95/5	1.017	27.7	0.232
90/10	1.022	29.3	0.188
85/15	1.024	23.35	0.103
80/20	1.029	23.40	0.109
0/100	1.030	2.7	0.220

The ultimate properties calculated from this figure, namely the elongation at break,  $\alpha_r$ , the nominal stress at break,  $f_r^*$ , and the energy required to break the samples,  $E_r$ , as a function of PLA concentration ( $\phi_{PLA}$ ) are shown in figure 5-7 and listed in Table 2. The energy required to break the samples was calculated by considering the area under the nominal stress-strain isotherms for the respective samples. The results clearly demonstrated that the flexibility of PLA was improved with the addition of CA, while the ultimate stress and energy required to break the samples have slightly declined with more CA added to the blend. This is interesting since FTIR spectral analysis indicated the formation of hydrogen bonding, which in fact should limit the extensibility of PLA chains. However, it is well known that the addition of hydrophilic polymers such as poly(ethylene glycol) act as plasticizers and diffuse in-between PLA chains and thus increase their extensibility. It is believed here as well that the 20% CA has acted in a similar way as to interact with the PLA chains and break its coagulation and thus cause its marked extensibilities. Further increase in the CA concentration as was mentioned contribute to the segregation of the two polymers leading to a decrease in the hydrogen bonding density and contributing further to the decline of the mechanical response of the polymeric blend.

**3.4. Dry thermal degradation measurements.** In order to evaluate the influence of the addition of CA polymer on the thermal stability of the PLA matrix, dry thermal degradation experimentation was conducted as described earlier. Results of the thermal degradation measurements are shown in Table 3 in terms of the ultimate mechanical properties, elongation at break, nominal force at break and the energy required to break the samples for different PLA/CA samples, namely 100/0 (Neat PLA), 90/10, 85/15 and 80/20 blend compositions. It is obvious from the table that the addition of CA polymer in general has improved the thermal stability of PLA with degradation. Blend compositions of 10% and 15% CA showed slight improvement in the blend extensibility with degradation but lower extensibility for the 20%

CA blend. Samples with more than 20% have failed the stress-strain test completely. The nominal force (stress) showed appreciable improvement when CA was added to the PLA matrix.

**Table 3.** Ultimate mechanical properties of PLA/CA blends before (ND) and after (D) accelerated thermal degradation at 50°C for 4 hrs

PLA/CA	$\alpha_r$		$f_r^*$ (N.mm <sup>-2</sup> )		$E_r$ (J.mm <sup>-3</sup> )	
	ND	D	ND	D	ND	D
100/0*	1.020	-	36.84	-	0.33	-
90/10	1.022	1.031	29.3	26.32	0.188	0.419
85/15	1.024	1.032	23.35	18.15	0.103	0.165
80/20	1.029	0.100	23.40	20.17	0.109	0.041

\*Degraded pure PLA sample were extremely weak and fragile to be subjected to stress-strain measurements

While neat PLA samples were too weak and fragile, upon degradation, to be subjected to the stress-strain test, PLA/CA blend samples showed nominal stress values that were slightly less than that of the non-degraded samples. The nominal force of the blend samples decreased with the increase in the CA content as was the case with the non-degraded samples. Interestingly, for the energy required to break the samples, the degraded 90/10 blend sample showed much higher values than those of the non-degraded sample. To elaborate on this point further, the influence of the extent of degradation on the mechanical response of the blend samples was studied. The 80/20 blend was subjected to an accelerated thermal degradation for an extended period of time at increasing degradation temperature. The results of this study are shown in Table 4.

**Table 4.** Degradation profile of PLA/CA 80/20 blend showing the influence of extended degradation on its ultimate mechanical properties.

Sample	Degradation Temperature(°C)	Degradation Period (hr)	$\alpha_r$	$f_r^*$ (N.mm <sup>-2</sup> )	$E_r$ (J.mm <sup>-3</sup> )
1*	-	-	1.029	23.4	0.109
2	50	4	1.032	18.15	0.041
3	100	24	1.018	16.01	0.025
4	100	48	1.008	8.54	0.014

\*Sample was not subjected to any degradation and was provided only for comparison with other samples

The results clearly show that the extended degradation period didn't affect the elongation at break to a great extent. Interestingly, the behavior of the nominal force with extended degradation showed a decrease in the nominal force at the early stages of the degradation (up to 4 hrs and 50°C) as expected. However after 24 hrs of the degradation at the high temperature at 100°C, the elongation at break, the nominal force and the energy required to break the sample have all increased considerably, thus indicated an increased toughness of the sample. This could be explained on the basis of crosslinking that might have taken place between the resultant free radicals produced from the degradation process and the polymeric chains thus causing the increase in the molecular weight of the samples, its crosslink density and over all high toughness. Further degradation (up to 48 hrs) has eventually degraded the samples and deteriorated its mechanical response.

**3.5. Molecular Modeling of the PLA/CA blend.** The molecular simulation techniques employed in this study combined a modified Flory-Huggins model to calculate the compatibility of binary mixtures. Two important extensions to the original Flory-Huggins model are employed:<sup>[34], [35]</sup>

- An explicit temperature dependence on the interaction parameter is employed herewith. This is accomplished by generating a large number of pair configurations and calculating the binding energies, followed by temperature



averaging the results using the Boltzmann factor and calculating the temperature-dependent interaction parameter.

- An off-lattice calculation, meaning that molecules are not arranged on a regular lattice as in the original Flory-Huggins theory, is also employed. The coordination number is explicitly calculated for each of the possible molecular pairs using molecular simulations.

By substituting the temperature-dependent interaction parameter,  $\chi$ , in the Flory-Huggins expression, the free energy is calculated for all compositions and temperatures. From this, the phase diagram of the mixture was determined and plotted in figures 8 and 9. Figure 8 clearly shows the impact of the molecular microstructure and the composition of the polymeric blends on the enthalpy of mixing PLA with CA as a function of the temperature. It is quite revealing from this chart that the enthalpy of mixing around room temperature had negative values indicating an exothermic mixing process leading to a polymeric blend stability. At both quite lower and quite higher temperatures, the enthalpy of mixing shows positive values pointing at possible microphase separation of the polymeric chains and an overall blend instability as the entropic contribution to the free energy of mixing may not be sufficient to overcome the enthalpic driven phase separation and could eventually result in the blend phase separation at these

temperatures in accordance with the following free energy expression:[36]

$$\Delta G = \Delta H - T\Delta S \quad (4)$$

To elaborate further on this point, the free energy of mixing was calculated following Eqn. 1 and was plotted in figure 9 against the mole composition of CA at various temperatures. It is quite interesting to observe here, in accordance with results obtained from figure 8, that the free energy of mixing showed positive values indicating phase separation at low temperatures. This could be explained on the basis that at low temperatures, the term  $T\Delta S$  is not large enough to overcome the positive  $\Delta H$  values in Eqn. 4 and the overall free energy is showing positive values. However, at quite high temperatures, the  $T\Delta S$  term is quite large not only to overcome the positive  $\Delta H$  values in Eqn. 4 but also to produce large negative values for the overall free energy of mixing indicating phase mixing at these temperatures even though the enthalpy of mixing had shown positive values at these temperatures. Another interestingly observation in figure 9 is the minima observed for the free energy of mixing at higher PLA compositions, which coincides with the experimental observations that blend compositions with higher PLA content had shown appreciable mechanical response whereas those with low PLA content had shown no mechanical integrity and couldn't be subjected to the stress-strain test due to their blend instability as predicted by the molecular simulation.

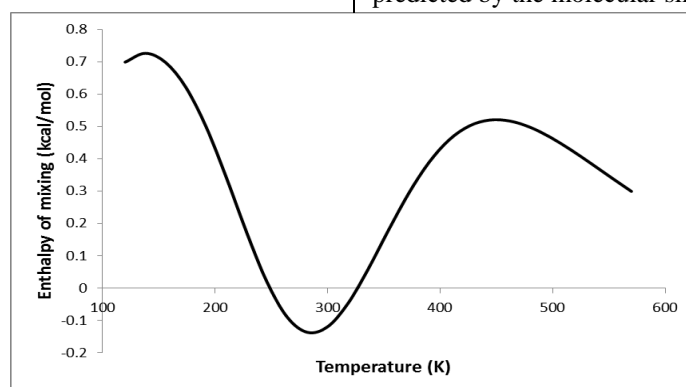


Figure 8. The influence of the temperature on the enthalpy of mixing PLA with CA polymer.

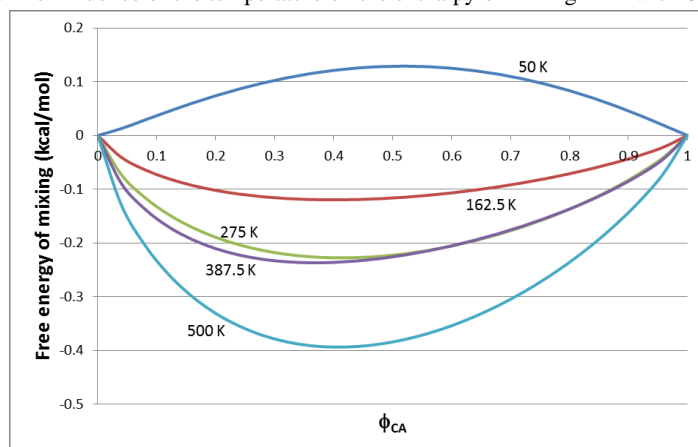


Figure 9. Phase diagram of PLA and CA polymeric blends showing the influence of temperature and composition on the free energy of mixing.

#### 4. CONCLUSIONS

One of the most promising “environmentally friendly” materials currently emerging as an alternative for the polluting petroleum-based polymers is poly(lactic acid) (PLA) as its biodegradability, low cost, high-speed production and good

mechanical performance make it suitable for a number of engineering applications. However, its stiffness and limited extensibility as well as its low thermal stability hinder its applicability in other applications. To improve on these properties,

blends of PLA and CA are considered. Issues such as influence of operating temperatures, suitable compositions and resistance to extended thermal degradation is investigated both experimentally and on a molecular-level using molecular modeling techniques to develop the underlying principles that influence the relationship between the blend microstructure and its macroscopic properties. The mechanical testing of the various blends showed that the addition of small amount of CA to PLA matrix has contributed to the flexibility of the blends while maintaining high values for the stress and thus leading to an improved overall toughness of these materials. Further increment in the CA component has reversed this trend and at 50% composition the samples completely failed the stress-strain test. The improved flexibility of 20% CA blend actually signifies the stability of the blend possibly due to the formation of 3D hydrogen bonding network between CA and PLA chains as indicated by FTIR spectral analysis. At higher CA concentrations, the repulsive forces between the two slightly hydrophobic polymers increase greatly up to the point that they could not be stabilized by the formation of the hydrogen bonds and blends. While TGA thermograms of the various PLA/CA blend films showed steady degradation behavior as a common feature, extended thermal degradation, on the other hand, highlighted the susceptibility of neat PLA to degradation over extended periods of time, which indicates that the degradation process of PLA is rather a slow one and that the presence of CA component in these blends has, in fact, protected the PLA chains.

The presence of small portions of CA has actually improved the mechanical response of the degraded blends in contrast to that of the degraded neat PLA samples, which could be explained on the basis of crosslinking that might have taken place between the resultant free radicals produced from the degradation process and the polymeric chains, thus causing the increase in the molecular weight of the samples, its crosslink density and over all increased toughness. Another interesting conclusion is that these materials, which could be extruded and shaped easily as they are simply mixed, by time its mechanical properties during normal operation conditions will continue to improve due to the slow crosslinking process resulting from the material ageing. Molecular simulation techniques revealed that the enthalpy of mixing around room temperature had negative values indicating an exothermic mixing process leading to blend stability. At lower and higher temperatures an endothermic mixing process has occurred indicating possible blend instability especially at low temperatures as the entropic contribution to the free energy of mixing is not sufficient to overcome the enthalpic-driven phase separation. The greater negative  $\Delta G$  values at higher PLA compositions also coincided with the experimental observations that blends composition with higher PLA portions had shown considerable mechanical response whereas those with higher CA content showed no mechanical integrity and couldn't be subjected to the stress-strain test due to their blend instability as predicted by the molecular simulation.

## 5. REFERENCES

- [1] Y. Khane, B. Lahcene, M. Benali, Synthesis, characterization of poly of poly(ester-amide) biodegradable and evaluation of their antimicrobial activity, *Biointerface Res. Appl. Chem.*, 6, 2, 1104–1111, **2016**.
- [2] M. Jamshidian, E. A. Tehrani, M. Imran, M. Jacquot, and S. Desobry, Poly-Lactic Acid: production, applications, nanocomposites, and release studies, *Compr. Rev. Food Sci. Food Saf.*, 9, 5, 552–571, **2010**.
- [3] A. Maazouz, K. Lamnawar, and B. Mallet, Compounding and processing of biodegradable materials based on PLA for packaging applications: In greening the 21st century materials world, *Front Sci Eng*, 1, 1–44, **2011**.
- [4] V. P. Martino, A. Jiménez, and R. A. Ruseckaite, Processing and characterization of poly(lactic acid) films plasticized with commercial adipates, *J. Appl. Polym. Sci.*, 112, 4, 2010–2018, May **2009**.
- [5] D. Garlotta, A literature review of poly (lactic acid), *J. Polym. Environ.*, 9, 2, 63–84, **2001**.
- [6] M. C. Gupta and V. G. Deshmukh, Radiation effects on poly (lactic acid), *Polymer*, 24, 7, 827–830, **1983**.
- [7] F.-D. Kopinke, M. Remmler, K. Mackenzie, M. Möder, and O. Wachsen, Thermal decomposition of biodegradable polyesters—II. Poly (lactic acid), *Polym. Degrad. Stab.*, 53, 3, 329–342, **1996**.
- [8] V. Taubner and R. Shishoo, Influence of processing parameters on the degradation of poly(L-lactide) during extrusion, *J. Appl. Polym. Sci.*, 79, 12, 2128–2135, **2001**.
- [9] S.-H. Hyon, K. Jamshidi, and Y. Ikada, Effects of residual monomer on the degradation of DL-lactide polymer, *Polym. Int.*, 46, 3, 196–202, **1998**.
- [10] A. Södergård and J. H. Näsman, “Stabilization of poly (L-lactide) in the melt,” *Polym. Degrad. Stab.*, 46, 1, 25–30, **1994**.
- [11] F. Signori, M.-B. Coltelli, and S. Bronco, Thermal degradation of poly (lactic acid)(PLA) and poly (butylene adipate-co-terephthalate)(PBAT) and their blends upon melt processing, *Polym. Degrad. Stab.*, 94, 1, 74–82, **2009**.
- [12] H. J. Lehermeier and J. R. Dorgan, Melt rheology of poly (lactic acid): Consequences of blending chain architectures, *Polym. Eng. Sci.*, 41, 12, 2172–2184, **2001**.
- [13] F. La Mantia, *Handbook of plastics recycling*. iSmithers Rapra Publishing, **2002**.
- [14] Y. Di, S. Iannace, E. D. Maio, and L. Nicolais, Poly(lactic acid)/organoclay nanocomposites: Thermal, rheological properties and foam processing, *J. Polym. Sci. Part B Polym. Phys.*, 43, 6, 689–698, Mar. **2005**.
- [15] J. Kylmä and J. V. Seppälä, Synthesis and characterization of a biodegradable thermoplastic poly (ester- urethane) elastomer, *Macromolecules*, 30, 10, 2876–2882, **1997**.
- [16] M. Villalobos, A. Awojulu, T. Greeley, G. Turco, and G. Deeter, Oligomeric chain extenders for economic reprocessing and recycling of condensation plastics, *Energy*, 31, 15, 3227–3234, **2006**.
- [17] B.-H. Li and M.-C. Yang, Improvement of thermal and mechanical properties of poly(L-lactic acid) with 4,4-methylene diphenyl diisocyanate, *Polym. Adv. Technol.*, 17, 6, 439–443, **2006**.
- [18] E. L. Teoh, M. Mariatti, and W. S. Chow, Thermal and Flame Resistant Properties of Poly (Lactic Acid)/Poly (Methyl Methacrylate) Blends Containing Halogen-free Flame Retardant, *Procedia Chem.*, 19, 795–802, **2016**.
- [19] F. Awaja, F. Daver, E. Kosior, and F. Cser, The effect of chain extension on the thermal behaviour and crystallinity of reactive extruded recycled PET, *J. Therm. Anal. Calorim.*, 78, 3, 865–884, **2004**.
- [20] Y. Wang, C. Fu, Y. Luo, C. Ruan, Y. Zhang, and Y. Fu, Melt synthesis and characterization of poly(L-lactic acid) chain linked by multifunctional epoxy compound, *J. Wuhan Univ. Technol.-Mater Sci Ed*, 25, 5, 774–779, Oct. **2010**.
- [21] S. Pilla, S. G. Kim, G. K. Auer, S. Gong, and C. B. Park, Microcellular extrusion-foaming of polylactide with chain-extender, *Polym. Eng. Sci.*, 49, 8, 1653–1660, **2009**.
- [22] Y.-M. Corre, A. Maazouz, J. Duchet, and J. Reignier, Batch foaming of chain extended PLA with supercritical CO<sub>2</sub>: Influence of the rheological properties and the process parameters on the cellular structure, *J. Supercrit. Fluids*, 58, 1, 177–188, **2011**.
- [23] M. Mihai, M. A. Huneault, and B. D. Favis, Rheology and extrusion foaming of chain-branched poly(lactic acid), *Polym. Eng. Sci.*, 50, 3, 629–642, **2010**.

- [24] L. Petersson and K. Oksman, Biopolymer based nanocomposites: Comparing layered silicates and microcrystalline cellulose as nanoreinforcement, *Compos. Sci. Technol.*, 66, 13, 2187–2196, **2006**.
- [25] E. L. Teoh, M. Mariatti, and W. S. Chow, Thermal and Flame Resistant Properties of Poly (Lactic Acid)/Poly (Methyl Methacrylate) Blends Containing Halogen-free Flame Retardant, *Procedia Chem.*, 19, 795–802, **2016**.
- [26] T. M. Madkour and R. A. Azzam, Use of blowing catalysts for integral skin polyurethane applications in a controlled molecular architectural environment: Synthesis and impact on ultimate physical properties, *J. Polym. Sci. Part Polym. Chem.*, 40, 14, 2526–2536, **2002**.
- [27] M. Kowalczyk, E. Piorkowska, P. Kulpinski, and M. Pracella, Mechanical and thermal properties of PLA composites with cellulose nanofibers and standard size fibers, *Compos. Part Appl. Sci. Manuf.*, 42, 10, 1509–1514, **2011**.
- [28] R. Masirek, Z. Kulinski, D. Chionna, E. Piorkowska, and M. Pracella, Composites of poly(L-lactide) with hemp fibers: Morphology and thermal and mechanical properties, *J. Appl. Polym. Sci.*, 105, 1, 255–268, **2007**.
- [29] E. Fortunati, D. Puglia, J. M. Kenny, M. M.-U. Haque, and M. Pracella, Effect of ethylene-co-vinyl acetate-glycidylmethacrylate and cellulose microfibrils on the thermal, rheological and biodegradation properties of poly (lactic acid) based systems, *Polym. Degrad. Stab.*, 98, 12, 2742–2751, **2013**.
- [30] O. Faruk, A. K. Bledzki, H.-P. Fink, and M. Sain, Progress Report on Natural Fiber Reinforced Composites: Progress Report on Natural Fiber Composites, *Macromol. Mater. Eng.*, 299, 1, 9–26, **2014**.
- [31] T. Madkour and J. E. Mark, Elastomeric properties of poly (dimethylsiloxane) networks having bimodal and trimodal distributions of network chain lengths, *Macromol. Rep.*, 31, 1–2, 153–160, **1994**.
- [32] T. M. Madkour and M. S. Hamdi, Elastomers with two crosslinking systems of different lengths viewed as bimodal networks, *J. Appl. Polym. Sci.*, 61, 8, 1239–1244, **1996**.
- [33] T. M. Madkour, Dynamical simulated annealing for assessing the high performance nature of poly (ethersulfone) s, *Angew. Makromol. Chem.*, 266, 1, 63–69, **1999**.
- [34] T. M. Madkour and J. E. Mark, Simulations on crystallization in stereoblock poly (propylene). Idealized structures showing the effects of atactic block length, *Macromol. Theory Simul.*, 7, 1, 69–77, **1998**.
- [35] T. M. Madkour and J. E. Mark, Mesoscopic modeling of the polymerization, morphology, and crystallization of stereoblock and stereoregular polypropylenes, *J. Polym. Sci. Part B Polym. Phys.*, 40, 9, 840–853, **2002**.
- [36] T. M. Madkour, A combined statistical mechanics and molecular dynamics approach for the evaluation of the miscibility of polymers in good, poor and non-solvents, *Chem. Phys.*, 274, 2, 187–198, **2001**.

## 6. ACKNOWLEDGEMENTS

The first author would like to acknowledge the support received from the Academy for Scientific Research and Technology (ASRT), Egypt, through the Grant ASR/SNG/W/2014–9 and the third author acknowledges the support he received from the American University in Cairo through the research grant FY15/51 both were absolutely monumental to complete the study.

© 2017 by the authors. This article is an open access article distributed under the terms and conditions of the Creative Commons Attribution license (<http://creativecommons.org/licenses/by/4.0/>).